Author for correspondence:
Mahdi Moradian,
E-mail: moradianpour@gmail.com

CAMBRIDGE
UNIVERSITY PRESS

Employing the dumbbell-shaped longitudinal slot antennas in the planar slotted antenna arrays

Mahdi Moradian [ID]

Department of Electrical Engineering, Lenjan Branch, Islamic Azad University, Isfahan, Iran

Abstract

The dumbbell-shaped longitudinal slot antennas are employed as a replacement for the round-ended longitudinal slot antennas. Each dumbbell-shaped slot is excited by an iris and a septum that have offsets from the waveguide centerlines. All the slots are also cut along the waveguide centerlines. It is demonstrated that the resonant length of the proposed dumbbell-shaped slot antennas is much smaller than the round-ended longitudinal slot antennas. Hence, the end-to-end spacings between the adjacent radiating slots as well as the end-to-end spacings between the coupling and the radiating slots increased noticeably in comparison with the arrays consist of the round-ended longitudinal slot antennas. This fact indicates that one can neglect the mutual coupling between the neighboring slots that are associated with the exciting higher-order modes at the slot positions. To better demonstrate the effectiveness of the proposed dumbbell-shaped slot antennas, a planar array antenna consists of the proposed dumbbell-shaped slot antennas have been designed, implemented, and tested. The measurement and the simulation results confirm the effectiveness of the proposed slot antennas.

Introduction

Waveguide fed longitudinal slot arrays play an essential role in radars and communication systems. They provide unique features that are of interest to many antenna designers. High efficiency, linear polarization, incorporating feeding and radiating systems, high power handling, and mechanical rigidity are some of their advantageous [1–8]. Despite these advantages, the waveguide fed longitudinal slot antennas have a main shortcoming. The shortcoming is attributed to the alternating offsets of the neighboring slots in the arrays. The alternating offsets of the neighboring slots introduce some undesirable lobes to the radiation patterns of the antennas which are usually called the butterfly lobes or second-order beams [9–12]. Several techniques have been proposed to eliminate these undesirable lobes which are effective in eliminating or suppressing these undesirable lobes [13–39].

In addition to the shortcoming mentioned above, one who wants to design such kinds of slot antennas has usually encountered another difficulty, which is associated with the excited higher-order modes at the positions of each slot or junction. For the rectangular waveguide fed the longitudinal slot antennas, the coupling between the neighboring slots associated with the exciting TE20 mode at the position of each slot has been investigated by developing some analytical design equations [40, 41]. In the planar slotted array antennas, the waveguides containing the radiating slots (branch line waveguides) are usually fed from underneath by centered inclined slots (coupling slots). It has been shown that for the slotted array antennas fed by inclined coupling slots from behind, the excited higher-order modes at the junctions contribute noticeably to the excited voltage at the neighboring radiating slots [42, 43]. Hence, in the high-performance slotted arrays, not the input impedance matching nor the desired radiation pattern specifications can be achieved [42, 43] if one just for simplicity neglects these exciting higher-order modes in the design procedure. Although it is possible to include the effect of the exciting higher-order modes at the junctions to the design equations, for many cases, performing these calculations can be quite cumbersome and time-consuming [44–46].

The dumbbell-shaped slots have been employed to design the slotted array antennas since several decades earlier [8]. It was also well-understood that the resonant length of the dumbbell-shaped slot antennas is much smaller than the round-ended slot antennas [8, 47, 48]. However, such type of slot antennas was mainly employed because of their more straightforward realization as well as the higher mechanical strength of the implemented antennas[8]. For avoiding confusion and clarifying the novelty of the idea presented in the current article, some explanations are required. The novelty of the idea presented in the article can be viewed from different aspects which is listed below

- The introduced dumbbell-shaped slot antennas in the current article are excited by the combination of irises and septums. In contrast with the dumbbell-shaped slot antennas fed by the rectangular waveguide which for the small offsets, the admittance cannot be controlled in an appropriate dynamic range [48], in the proposed dumbbell-shaped slot antennas, the admittance of the antennas can be controlled in a wide dynamic range. The simulation results have shown that for the proposed antennas, the equivalent normalized self-conductance can be easily controlled from zero up to one by increasing the iris depth. In the same manner, for any iris depth, the equivalent normalized self-susceptance of the antennas can be controlled approximately from −60% up to 60% of the associated equivalent normalized self-conductance by varying the slot length.
- An iterative design procedure is employed in the current article to design arrays consists of the proposed dumbbell-shaped slot antennas. Because the design procedure is straightforward and exact, both the internal and the external mutual couplings between the dumbbell-shaped slot antennas are taken into account. So, for the designed antennas based on the design procedure, the desired radiation pattern specifications, as well as the input impedance matching, are achieved.
- The article demonstrates by some examples that the smaller resonant length of the proposed dumbbell-shaped slot antennas which leads to the larger distances between the tips of the successive slots may be used as an advantage. These larger distances let one to ignore the effect of the exciting higher-order modes at the junctions on the excitation of the neighboring radiating slots. So, the required designing equations for the slotted antenna arrays consist of the dumbbell-shaped slot antennas can be obtained only by considering the data associated with the dominant mode solely which dramatically simplifies them.

    In the next sections, the proposed dumbbell-shaped slot antennas are introduced. The validity of their equivalent shunt admittance model is discussed. The designing graphs, as well as the designing equations, are derived. Finally, the performance of some arrays consists of the proposed dumbbell-shaped slot antennas will be demonstrated and discussed.

The proposed slot antennas

The proposed slot antenna, together with its various parameters, is depicted in Fig. 1. According to the figure, the shape of the slot
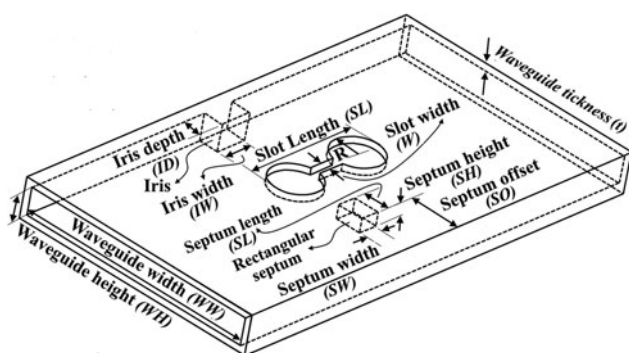
Fig. 1. Dumbbell-shaped slot antenna fed by the rectangular waveguide including its parameters.

is in the form of a dumbbell. For simple realization, the shape of the end parts is chosen to be circles. The width of the slot in the middle is denoted by W. R denotes the radius of the slot at both ends. Moreover, SL indicates the length of the slot. It is also worthy to note that the slot is placed along the waveguide center-line. For exciting the slot, an iris and a rectangular septum are placed at both sides of the slot. The rectangular septum has offset from the centerline. Furthermore, the symmetry plane of the iris and the septum bisects the slot. The feeding waveguide is also a reduced-height rectangular waveguide with an inside cross-section of 72 mm × 8 mm.

Because the dumbbell-shaped slot antennas have many parameters, it is not possible to investigate the characteristics of slot antennas without assigning values to some of their parameters. Please note that there is no frequency limitation on the proposed dumbbell-shaped slot antennas and they can be employed to design different arrays of slots at various frequencies. For this reason, hereafter the listed dimensions in Table 1 are considered to study the characteristics of the proposed dumbbell-shaped slot antennas. Besides, all the following simulations are done at 3 GHz.

It has been found that in the proposed dumbbell-shaped slot antennas, the septum length depends on the iris depth. To derive the appropriate septum length versus the iris depth, the procedure which has been offered in [49] was followed. Figure 2 shows the applicable septum length versus the iris depth. Overall, only the iris depth and the slot length are selected as variables to control the characteristics of the proposed dumbbell-shaped slot antennas.

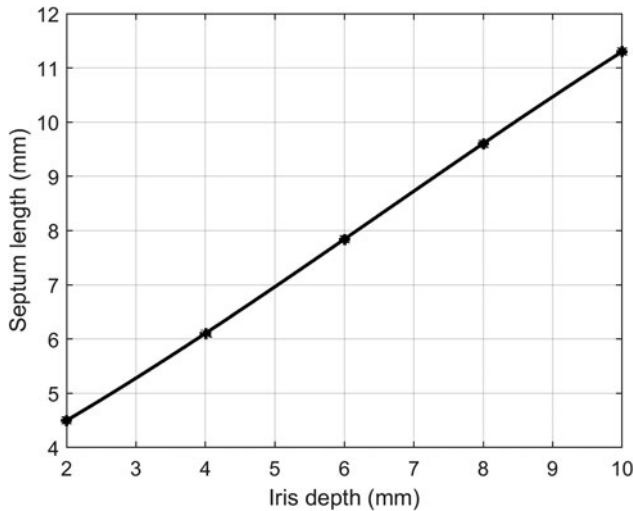## Deriving the design equations and studying their validity

The slotted array antennas consist of the longitudinal slots can be designed by employing two main design equations and following the iterative design procedure proposed by Elliott [40]. The provided design equations in [1, 40] cannot be directly employed to design an array composed of the proposed dumbbell-shaped slot antennas. So, it is crucial to obtain two new design equations similar to the design equations specifically proposed for the round-ended longitudinal slot antennas [1].

The design equations which have been presented by Elliott relay on one main assumption that the longitudinal slot antennas fed by the rectangular waveguides can be considered as an equivalent normalized admittance on a transmission line. Similarly, to establish the design equations for the proposed dumbbell-shaped slot antennas, first, it has to be shown that considering the antennas as a shunt admittance on a transmission line is valid. Hence, a model of the proposed dumbbell-shaped slot antennas was drawn in Ansys high-frequency structure simulator (HFSS). Two waveguide ports have been assigned to the model. The model has been bounded by some radiated boundaries.

The simulation of the model was done for various depths of the iris and different lengths of the slot. Then, the amplitudes of the forward- and backward-scattered waves were derived. The amplitudes and the phases of the forward- and backward-scattered waves for various iris depths and slot lengths are listed in Table 2. According to the table, for some slot lengths, the difference between the amplitude and the phase of the scattered waves is negligible. So, it is possible to model the proposed dumbbell-shaped slot antennas as an equivalent shunt admittance on a transmission line if one chose the slot length in an appropriate interval. However, for the slot length far from this appropriate interval, the shunt admittance modeling is a weak assumption.

Table 1. Dimensions of the proposed dumbbell-shaped slot antennas

Iris width (IW)	Septum width (SW)	Waveguide inner width (WW)	Waveguide inner height (WH)	Waveguide thickness (t)
10 mm	6 mm	72 mm	8 mm	2 mm
Slot width (W)	Dumbbell radios (R)	Septum height (SH)	Septum offset (SO)	
3 mm	15 mm	4 mm	20 mm	

Fig. 2. Proper septum length versus the iris depth.

Table 2. Scattered forward- and backward-mode amplitude and phase for various slot lengths and iris depths

Iris depth (mm)	Slot length (mm)	Scattered forward-mode amplitude and phase (°)	Scattered backward-mode amplitude and phase (°)
2	36.0	0.011∠-161	0.016∠-134
	37.0	0.0224∠-163	0.0245∠155
	38.0	0.0285∠173	0.0291∠173
	39.0	0.022∠156	0.025∠146
	40.0	0.013∠157	0.0192∠131
4	36.0	0.031∠-129	0.037∠-138
	37.0	0.0511∠-154	0.054∠150
	38.0	0.063∠178	0.063∠178
	39.0	0.053∠156	0.055∠151
	40.0	0.036∠143	0.042∠134
6	36.0	0.066∠-131	0.07∠-129
	37.0	0.096∠-149	0.098∠148
	38.0	0.12∠-176	0.12∠-177
	39.0	0.105∠158	0.11∠155
	40.0	0.08∠143	0.09∠137
8	36.0	0.105∠-130	0.11∠-128
	37.0	0.15∠-146	0.15∠-145
	38.0	0.189∠-170	0.189∠-170
	39.0	0.18∠165	0.18∠163
	40.0	0.15∠147	0.15∠144
10	36.0	0.15∠-129	0.16∠-126
	37.0	0.20∠-143	0.21∠-141
	38.0	0.26∠-164	0.26∠-162
	39.0	0.27∠177	0.27∠174
	40.0	0.24∠154	0.24∠154

As the table shows, for some iris depths, the phase of the scattered waves varies a lot even for small changes of the slot length. Please note that the proposed slot antennas are inherently narrowband. So, it is expected to see a large variation in the amplitude and the phase of the induced propagating waves. In [50], a similar large variation in the amplitude and the phase of the scattered waves is reported. It is known that in the slotted array antennas, the slot lengths are a few percents far from their self-resonant lengths [1]. So, the shunt admittance model can be employed to design different types of arrays consist of the proposed dumbbell-shaped slot antennas without much concern about the invalidity of the considered equivalent shunt admittance model.

It has been found worthy to study the transverse electric field distribution in the slot aperture [50]. For simulation, one-watt of electromagnetic power has been delivered to the antenna by one of the Wave-Ports, and the electric field in the slot was derived for two different iris depths. These iris depths were selected such that they lead to strong or weak radiations by the slot. Figure 3 shows the amplitude and the phase of the transverse electric fields in the slot against the normalized slot length for the iris depth equal to 2 and 10 mm and when the slot length was equal to 37.8 mm. The figure shows that the amplitude of the electric fields is almost constant in the middle part of the slot. It starts to drop sharply at the beginning of the circles and approaches zero at the ends of the slot. The phase of the transverse electric fields is almost constant in the most portion of the slot.

Figure 3 also shows that the amplitude of the induced voltage (the integration of the transverse electric field along the width of the slot) for the iris depth equal to 10 mm is much larger than the induced voltage for the iris depth equal to 2 mm. Because for both cases, the amplitudes of the transverse electric fields are

symmetrical in the slot aperture while their phases are more or less constant in the slot, it can be concluded again that the proposed dumbbell-shaped slot antennas at least at resonance can be represented as a shunt admittance on a transmission line [50].

To derived the design equations, the procedure proposed in [33] has been followed. First, the previously defined model in HFSS is developed by adding a lumped port to the middle of the slot. The model, including its details, is shown in Fig. 4. When the lumped port is excited, an electric field is developed in the slot aperture that in turn, this electric field excites two
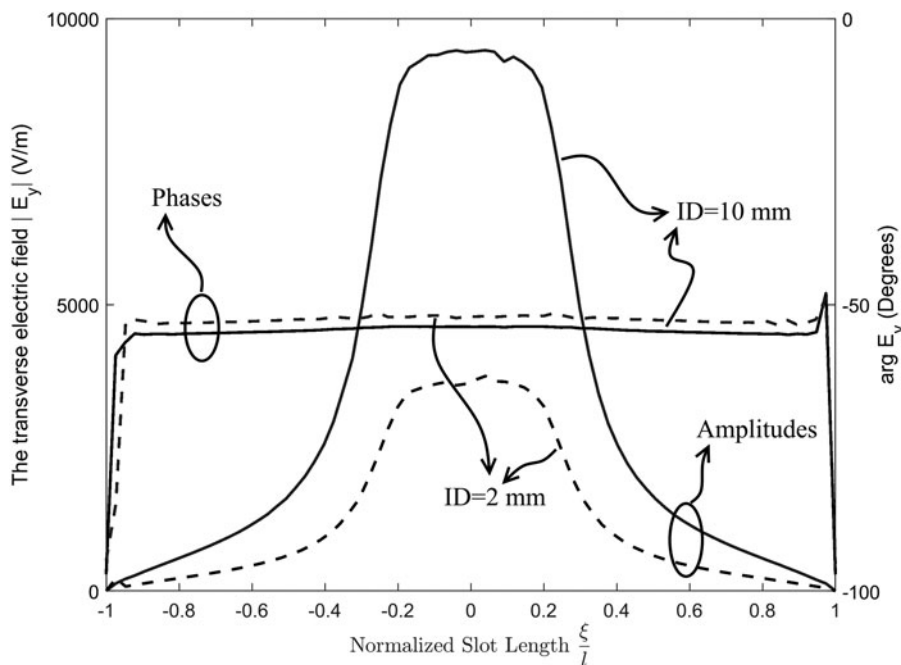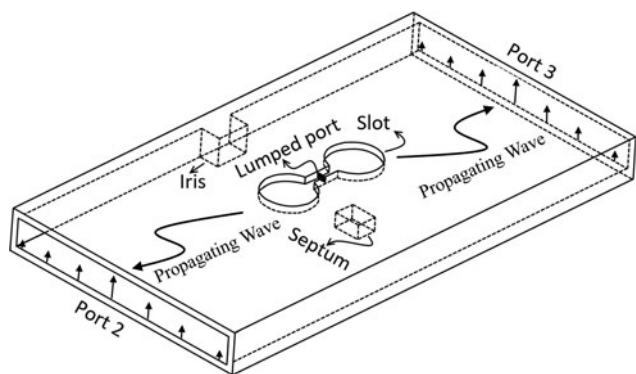
Fig. 4. Employed model to find the relation between the slot voltage and the amplitude of the induced waves.

outgoing propagating electromagnetic waves in the waveguide. The propagating waves and their polarization (although many electromagnetic modes are excited around the slot, it is supposed that only the dominant mode has appeared at output ports) are illustrated in Fig. 4. The developed transverse electric fields have been studied for the iris depths equal to 2 and 10 mm. It has been found that the discrepancy between the characteristics of the developed transverse electric fields along the slot was caused by both the impressed source (current model) and the internally incident wave that passed the slot (previous model) was negligible. The simulation results have also shown that for both cases, the phase of the fictional electric fields (the electric field which is caused by the lumped port) is almost constant. These facts indicate that the model can be employed to find the mathematical relationship between the slot voltage and the amplitudes of the forward- and backward-scattered waves.

The simulation of the model, shown in Fig. 4, has been carried out when the iris depth and the slot length were swept from 2 to 10 mm and 34 to 47 mm, respectively. Then, the scattering parameters were saved and analyzed. The slot voltage and the forward-

and back-ward-scattered wave amplitudes were derived from the scattering parameters of the model [33]. Finally, the following mathematical relation between the slot voltage and the amplitudes of the scattered waves of the nth slot was derived.

$$
\begin{aligned}
B_{10}^n = C_{10}^n &= -K f_n(x_n, l_n) V_n^s \\
&= 1.493 \times 10^{-5}(0.00247x^2 + 0.06x + 0.157)(0.0011l^2 \\
&\quad + 0.0202l - 0.0813) V_n^s
\end{aligned} \tag{1}
$$

In the above equation, x represents the iris depth, and l represents half of the slot length. Furthermore, B_{10}^n and C_{10}^n represent the amplitude of the forward- and backward-scattered waves. Besides, V_n^s is the voltage of the nth slot, and f_n is a function of the iris depth and the slot length. In [51], a design procedure was proposed to design slotted array antennas covered with a dielectric slab. Although the proposed design procedure was mainly aimed to design an array of the dielectric covered slotted arrays, without serious limitation, it can also be employed to design different types of slotted arrays including arrays consist of the dumbbell-shaped slot antennas. The design procedure uses two main design equations [51]. The first design equation is

$$
\frac{Y_n^a}{G_0} = K_1 f_n(x_n, l_n) \frac{V_n^s}{V_n} \tag{2}
$$

where V_n is the mode voltage in the equivalent network. Y_n^a/G_0 is the equivalent normalized active admittance of the nth slot [51]. Finally, K_1 can be derived as

$$
K_1 = \sqrt{4K^2 \omega \mu_0 \beta_{10}/G_0} \tag{3}
$$

where ω is the angular frequency. μ_0 is the free space permeability. β_{10} is the phase constant of the dominant mode, and G_0 is the characteristic admittance of the equivalent transmission line. Similarly, the second design equation can be derived from the
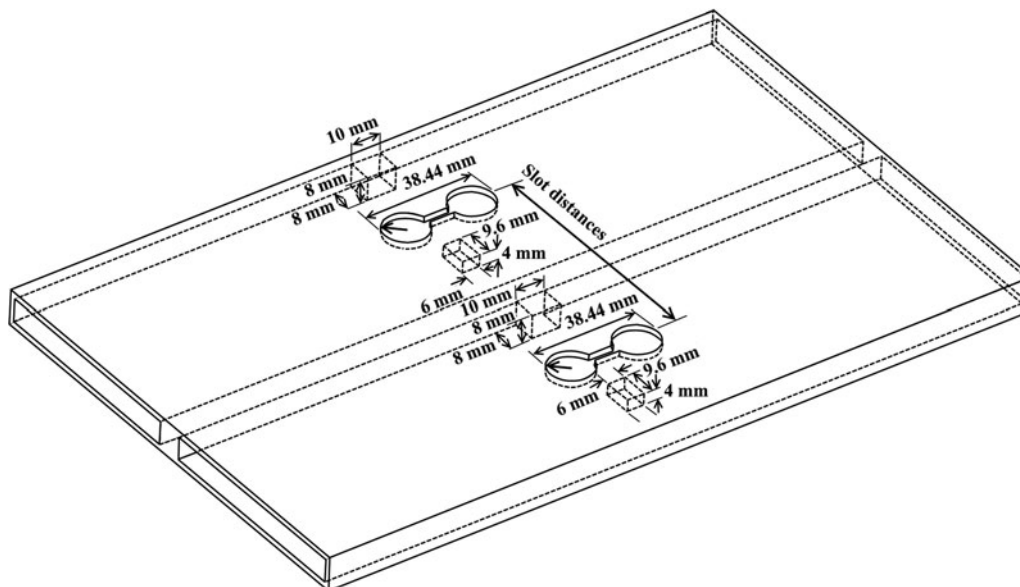
Fig. 5. Employed model to study the mutual coupling between the parallel slots.

procedure proposed in [51]

$$\frac{Y_n^a}{G_0} = \frac{K_2 f_n^2}{Y_n^{a'}}$$ (4)

where K_2 is equal to $4K^2\omega\mu_0\beta_{10}$, $Y_n^{a'}$ represents the active admittance of the nth loaded slot in the equivalent slotted array embedded in a very large ground plane.

To study the validity of design equations, the equivalent normalized active admittance of the proposed dumbbell-shaped slot antennas cut in the broad walls of two nearby rectangular waveguides are derived by HFSS and compared with the equivalent normalized active admittance which is derived by Eq. (4). Figure 5 shows the model which is used to obtain the equivalent normalized active admittance in HFSS. As seen by the figure, the slots are parallel and non-staggered (i.e. the longitudinal distance between the slots referred to a place bisects the slots is zero). The slot antennas are similar (i.e. all dimensions are the same). The slot lengths are equal to 38.44 mm, and the iris depths are equal to 8 mm. These selected dimensions ensure that each of the slot antennas resonates when the other slot is covered with a conducting tape or when the distance between the slots approaches infinity. The equivalent normalized self-admittances of the slot antennas are equal to 0.47. Four Wave-Ports were assigned to the model, and they have been de-embedded to the middle of the slot antennas. The simulation of the structure has been carried out when the spacing between the slots was swept from 76 mm to 526 mm. From the scattering parameters of the model, it is an easy task to find the equivalent normalized active admittance of the parallel slots [51].

To find the equivalent normalized active admittance from Eq. (4), a model which composed of a large circular conducting plane was drawn in HFSS IE. Two dumbbell-shaped slots were also cut into the conducting plane. Two lumped ports fed the slots at their middles and the model was parameterized. Figure 6 shows the model, including its different parameters. The model was then simulated to find the mutual admittance between the slots while the distance between the slots was swept from 76 mm to 526 mm. It is worthy to mention here that the author has only
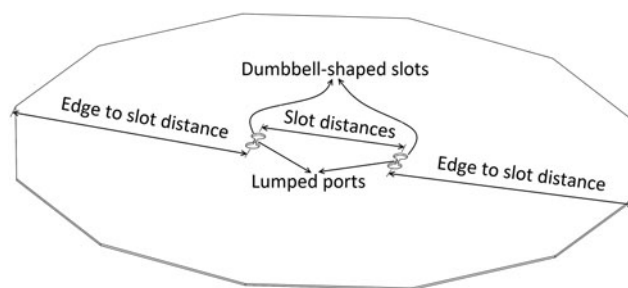

Fig. 6. Two parallel dumbbell-shaped slot embedded in the large circular ground plane.

used HFSS IE to derive the mutual admittance between the slots shown in Fig. 6 and all the other simulations have been carried out using HFSS. For any distance between the slots, the minimum spacing between the edge of the plane and the slots was always greater than seven times of the free-space wavelength (for our case 700 mm). Then, the estimated mutual admittance between the slots and the equivalent normalized self-admittance of the slots were used in Eq. (4) to find the equivalent normalized active admittance. Figure 7 shows the derived equivalent normalized active admittances against the normalized distance between the slots when the slots are parallel and non-staggered. As seen by the figure, the difference between the two approaches is negligible.

The defined models have been used again for comparing the normalized equivalent active admittance of the slot antennas when the slots are staggered by 0.5 and 1.0 guided wavelength. Figures 8 and 9 show the derived normalized equivalent active admittances of the slot antennas when they are staggered by one-half and one of the guided wavelength, respectively. As seen by the figures, the agreement between the results associated with two approaches is satisfactory. Based on the performed discussion, it can be concluded that Eq. (4) can be employed to predict the equivalent normalized active admittance of any slot in an antenna array consists of the proposed dumbbell-shaped slots with acceptable accuracy.
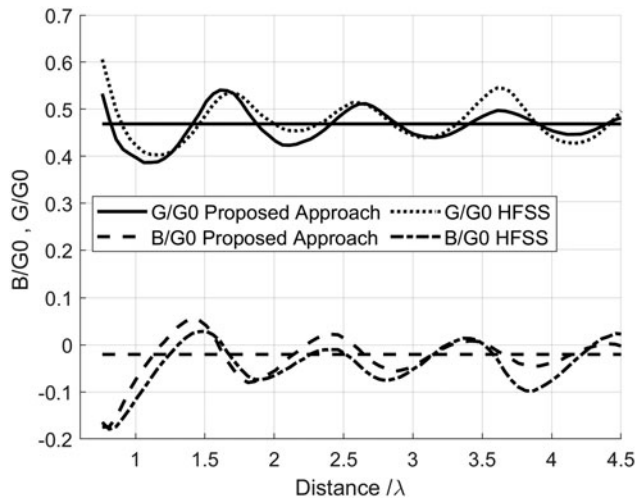
Fig. 7. Variation of the normalized active admittance of the coupled slot antennas versus the normalized distance when the slots are non-staggered.

Fig. 8. Variation of the normalized active admittance of the coupled slot antennas versus the normalized distance when the slots are staggered by one-half of the guided wavelength.
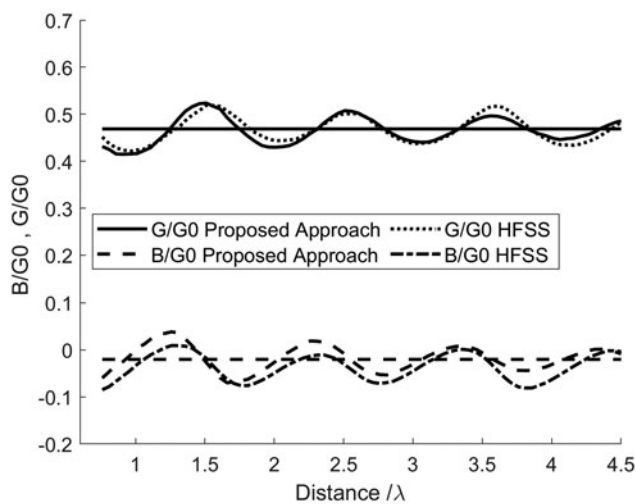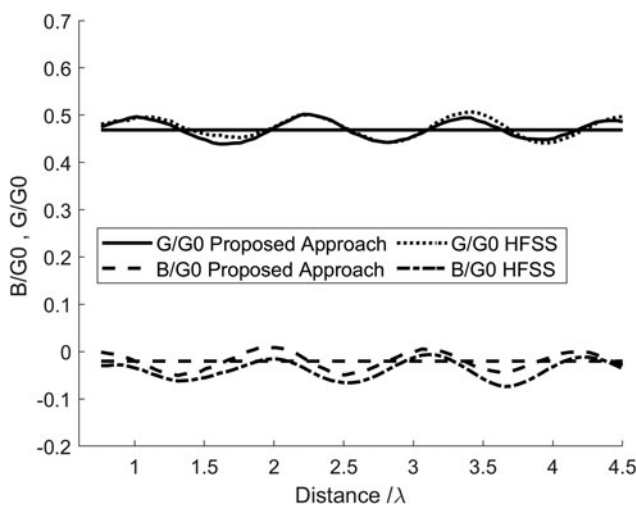

Fig. 9. Variation of the normalized active admittance of the coupled slot antennas versus the normalized distance when the slots are staggered by one guided wavelength.

Designing the slotted arrays of the dumbbell-shaped slot antennas and the results

To demonstrate the validity and effectiveness of the proposed dumbbell-shaped slot antennas, some slotted arrays have been designed. First, two standing wave slotted arrays consist of four waveguides and each waveguide contains four slots that have been designed and simulated. For the first array, all the antenna elements are centerline round-ended slots [49]. For the second array, the radiated elements are the proposed dumbbell-shaped slot antennas. For designing the arrays, the equivalent normalized self-admittance of the isolated slots (for both round-ended and dumbbell-shaped) must be known for every combination of the slot length and iris depth. For the round-ended slot, some universal curves have been derived that enable one to easily find the equivalent normalized self-admittance of the isolated slots [49]. Similarly, For the dumbbell-shaped slot antennas, it has been found that the equivalent normalized self-admittance of the isolated slots can be represented by some universal curves.

To find the universal curves for the dumbbell-shaped slot antennas, the predefined model in HFSS (Fig. 1) has been employed while the slot length and the iris depth in the model were swept from 17 to 23.5 mm and 2 to 10 mm, respectively. Then, the equivalent normalized shunt admittances, the resonant length, and resonant conductance of the dumbbell-shaped slot antennas for every combination of the slot lengths and iris depths were derived [49]. Figure 10 shows the resonant length times the free space wavenumber versus the iris depth. It is worthy to note that the resonant length of the proposed dumbbell-shaped slot antenna is much smaller than one-half of the free-space wavelength.

Figure 11 shows the resonant conductance versus the iris depth. As seen from the figure, the resonant conductance is an ascending function of the iris depth. The equivalent normalized self-conductance and susceptance of the proposed dumbbell-shaped slot antennas versus the normalized slot length, and for various iris depths are shown in Fig. 12. For ease of programming, two curves were also fitted over the data.

The arrays have been designed by employing the derived design equations and following the iterative procedure explained in [1, 4, 51]. A tilted slot in the primary feeding waveguide is
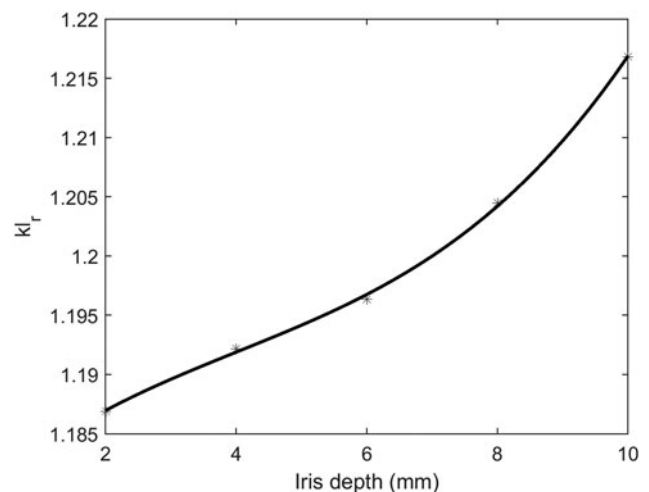

Fig. 10. Resonant length multiplied by the free space wavenumber versus the iris depth.
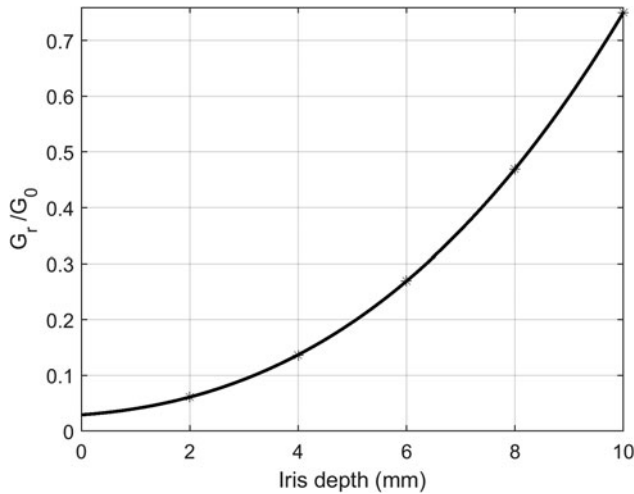
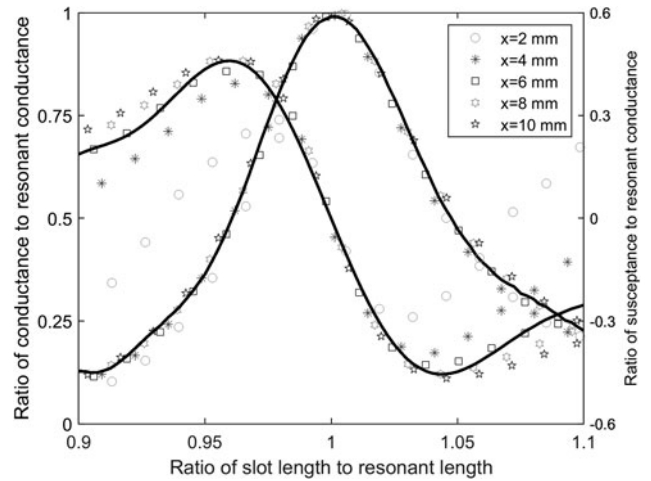**Fig. 11.** Normalized resonant conductance versus the iris depth.

Fig. 12. Normalized conductance and susceptance of the proposed slot antennas versus the normalized slot length.

used to feed each branch of the antennas. The input power is distributed by the ratio of 1:4.2:4.2:1 between the branches of the antennas. The prescribed power distribution has been achieved by tuning the tilts of the inclined slots while assuming that all the radiating slots are eliminated and the branch lines are terminated to matched loads.

The arrays have been designed to have Dolph–Chebyshev voltage distribution in both E- and H-planes with a sidelobe level of −20 dB in both planes. The top view of the first and the second design arrays are shown in Figs 13 and 14, respectively. At first glance, one can see that the distances between the edges of the coupling slots and edges of the nearest radiated slots are larger

Antenna dimensions in millimeter

Slot lengths				Iris widths				Iris depths				Septum widths			
Ls_1	Ls_2	Ls_3	Ls_4	Iw_1	Iw_2	Iw_3	Iw_4	Id_1	Id_2	Id_3	Id_4	Sw_1	Sw_2	Sw_3	Sw_4
50.5	51.1	49.5	50.4	10.0	10.0	10.0	10.0	5.9	8.5	6.7	10	6.0	6.0	6.0	6.0

Septum lengths				Lengths of the coupling slots		Tilts of the coupling slots		Other dimensions		
Sl_1	Sl_2	Sl_3	Sl_4	Lcs_1	Lcs_2	θ_1	θ_2	LS	W	T
4.2	4.8	6.2	7.7	56.5	53.47	9.0	20	74	65	10
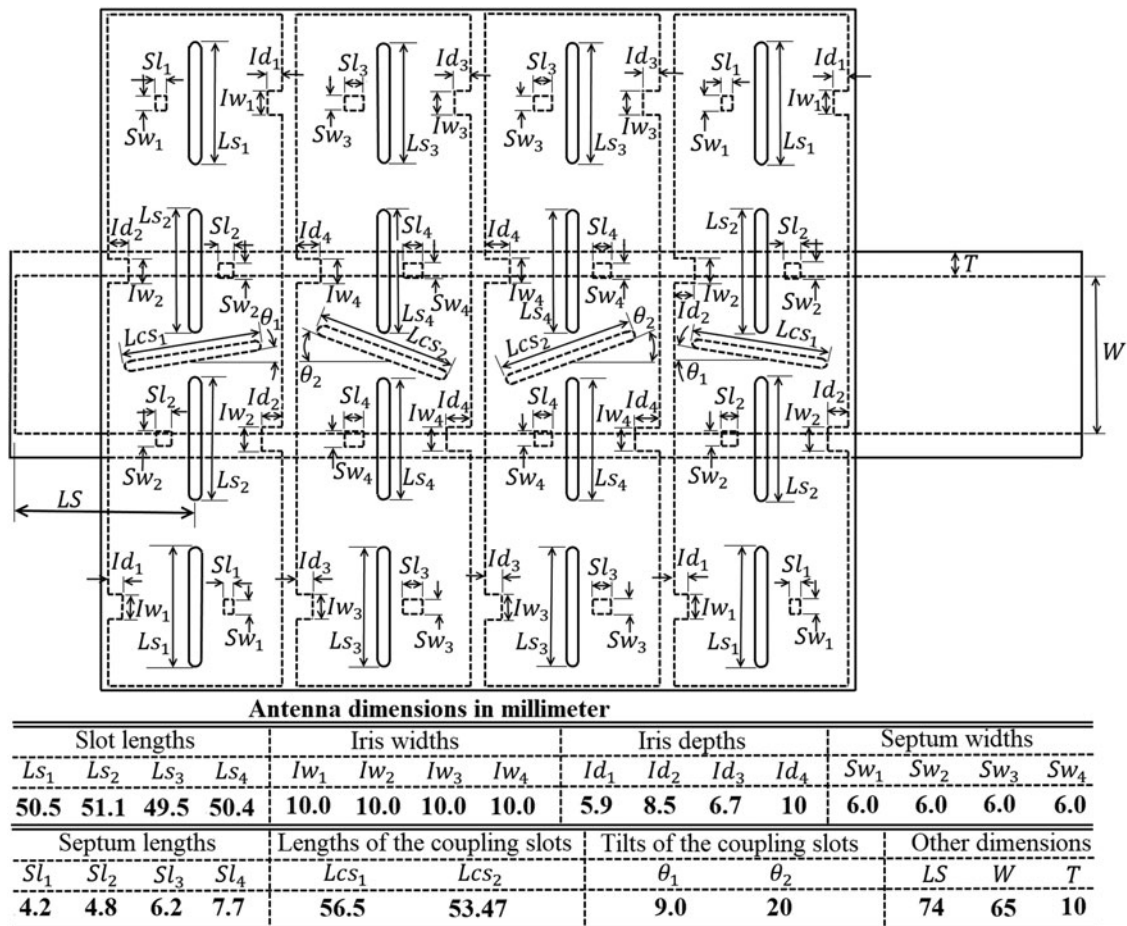
Fig. 13. Top view of the designed array consists of the round-ended slot antennas.

Antenna dimensions in millimeter

Slot lengths				Iris widths				Iris depths				Septum widths			
Ls_1	Ls_2	Ls_3	Ls_4	Iw_1	Iw_2	Iw_3	Iw_4	Id_1	Id_2	Id_3	Id_4	Sw_1	Sw_2	Sw_3	Sw_4
37.9	38	37.5	37.9	10.0	10.0	10.0	10.0	3.5	5.74	4.0	7.8	6.0	6.0	6.0	6.0

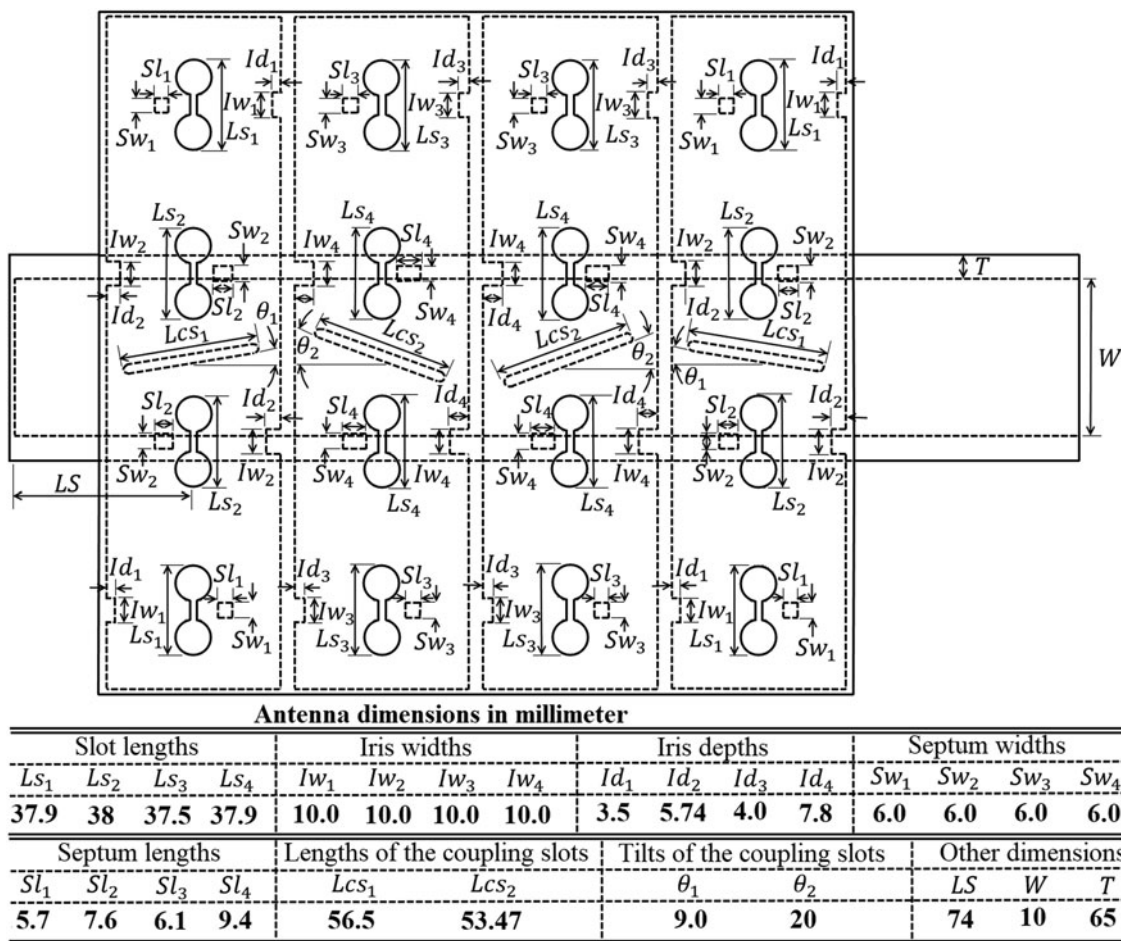| Septum lengths				Lengths of the coupling slots		Tilts of the coupling slots		Other dimensions		
Sl_1	Sl_2	Sl_3	Sl_4	Lcs_1	Lcs_2	θ_1	θ_2	LS	W	T
5.7	7.6	6.1	9.4	56.5	53.47	9.0	20	74	10	65

Fig. 14. Top view of the designed array consists of the proposed dumbbell-shaped slot antennas.

for the second array in comparison to the first array. This fact ensures that the internal higher-order modes exciting at the positions of the inclined slots will be suppressed enough before reaching to the neighboring radiating slots.

Figure 15 illustrates the reflection coefficients of the designed arrays versus frequency. The figure shows that for the first array,
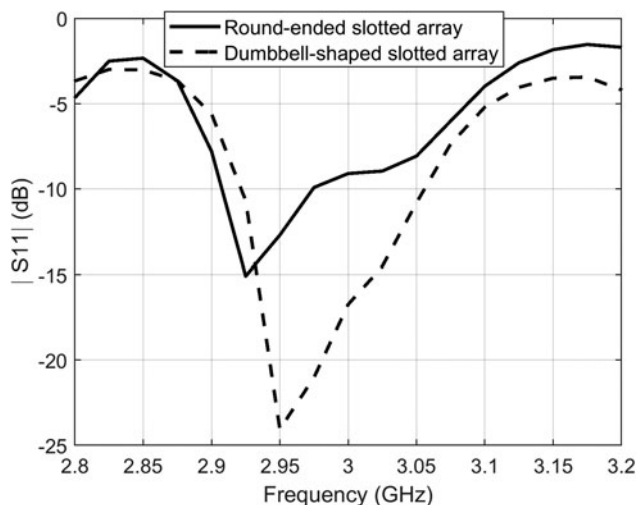
only in a small portion of the frequency band, the reflection coefficient is better than −10 dB. Whereas for the second array, the reflection coefficient is better than −10 dB from 2.95 to 3.05 GHz.

The co-polarization and cross-polarization radiation patterns of the arrays in both H- and E-planes are demonstrated in Figs 16 and 17, respectively. As the figure shows, the agreement
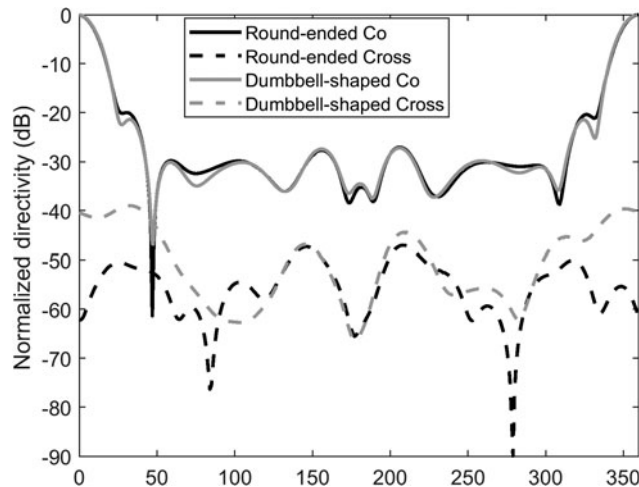

Fig. 15. Reflection coefficients of the designed arrays versus frequency.

Fig. 16. Radiation patterns of the designed antennas in the H-plane.
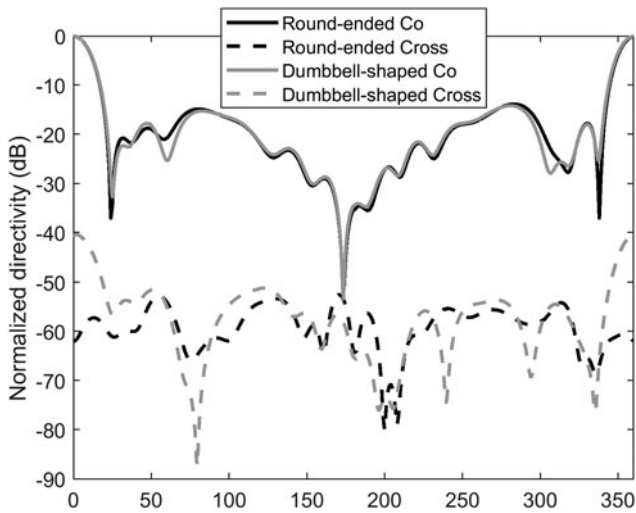
Fig. 17. Radiation patterns of the designed antennas in the E-plane.

Fig. 18. Different parts of the designed array together with its dimensions.

between the co-polarization radiation patterns is good. The cross-polarization radiation patterns of the designed antennas are also depicted in the figures. One can see from the figures that the discrepancy between the level of the cross-polarizations for the first and the second arrays is maximum at the direction of the main beam. However, the level of the cross-polarizations for both arrays at the direction of the main beam is better than −40 dB which is acceptable for most applications.

Although, the specifications of the designed slotted array antenna consists of the proposed dumbbell-shaped slots has been satisfactory, it was costly to construct a prototype. Hence, a smaller slotted array antenna has been designed to be implemented. The array is a standing wave array antenna contains eight dumbbell-shaped slot antennas. The array is designed to have Dolph–Chebyshev voltage distribution in H-plane with a sidelobe level of −20 dB. It also operates at S-band with the center frequency equal to 3 GHz. Figure 18 shows the different parts of the designed antenna, together with its various dimensions. As seen by the figure, the antenna has two waveguides, and there are four slots in each waveguide. An SMA connector feeds the main waveguide near one end. Then, the exciting electromagnetic wave feeds the branch line waveguides via the coupling slots. Photographs of different parts of the implemented antenna are shown in Fig. 19. The figure shows the feeding waveguide, the antenna body (branch line waveguides), and the complete assembled antenna.

Figure 20 shows the simulated and the measured reflection coefficient of the constructed antenna. As the figure shows, except for some frequency shift of the measured reflection coefficient, the results are in a good agreement. The measured reflection coefficient is better than −10 dB from 2760 to 3066 MHz. Whereas, the simulated reflection coefficient is better than −10 dB from 2855 to 3125 MHz. In addition, the measured reflection coefficient of the implemented antenna at the design frequency (3 GHz) is better than −12 dB. As the figure shows, an unwanted resonance appears in both the simulated and the measured reflection coefficients. One can see from the figure that there is a frequency shift between the unwanted resonances while the unwanted resonance in the measurement result is deeper.

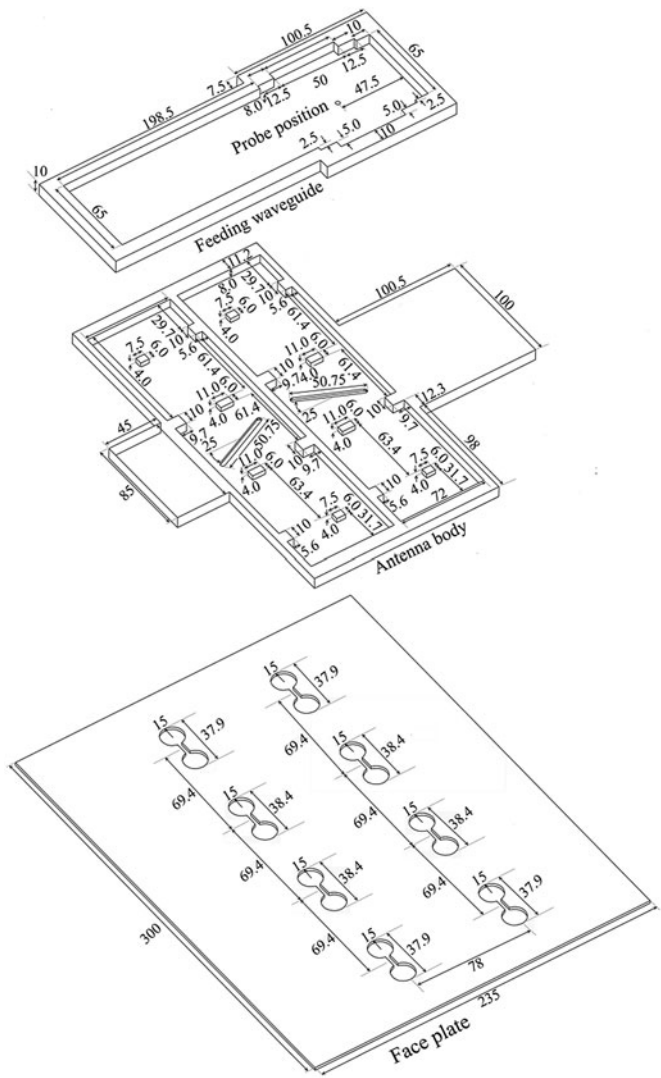The radiation patterns of the constructed antenna have been measured on the outdoor antenna test range. The simulated and the measured H-plane radiation patterns of the designed antenna are shown in Fig. 21. As seen from the figure, the agreement between the simulated and the measured radiation patterns is good. There is a small asymmetry in the level of the simulated innermost side-lobes, whereas the measured level of the innermost side-lobes is almost symmetrical. The figure also shows that for the innermost side-lobe, the prescribed specification for the side-lobe level is achieved. The simulated cross-polarization radiation pattern of the antenna is added to the figure. As the graph shows, the level of the cross-polarization at the direction of the main beam is approximately equal to −40 dB. The measured cross-polarization level at the direction of the main beam was approximate −26 dB below the co-polarization level. The difference between the simulated and the measured levels of the cross-polarization is due to the limited dynamic range of the available detector, which was used during the measurement.

The simulated and the measured radiation patterns of the designed antenna in E-plane are illustrated in Fig. 22. Although, the antenna is symmetrical, there is a small asymmetry in the radiation pattern which is due to the unequal power split between the antenna branches. As seen from the figure, the measured
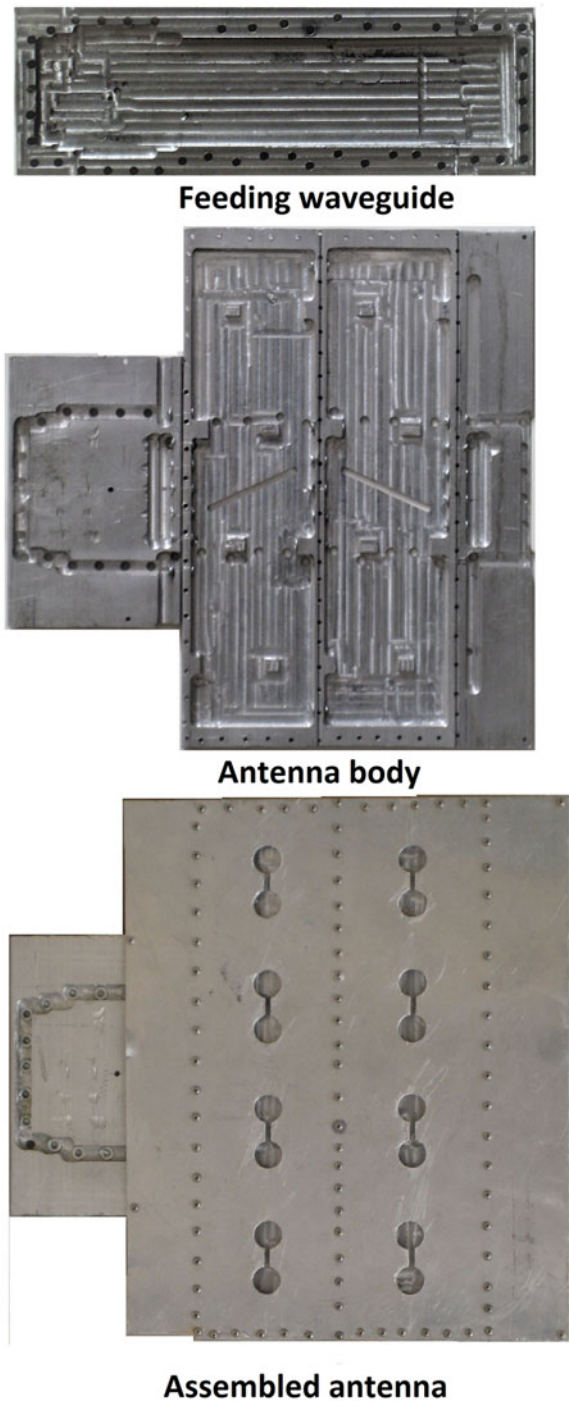
Feeding waveguide

Antenna body

Assembled antenna

Fig. 19. Photograph of the different parts of the implemented antenna.

Fig. 20. Simulated and measured reflection coefficients.
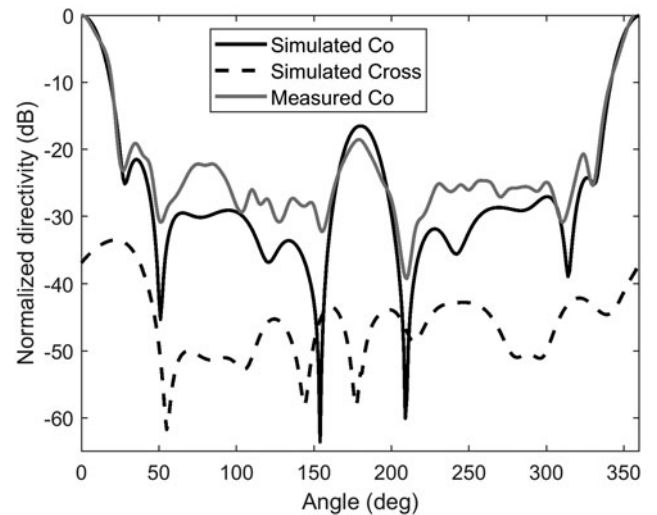
Fig. 21. Simulated and the measured radiation patterns of the implemented antenna in the H-plane.
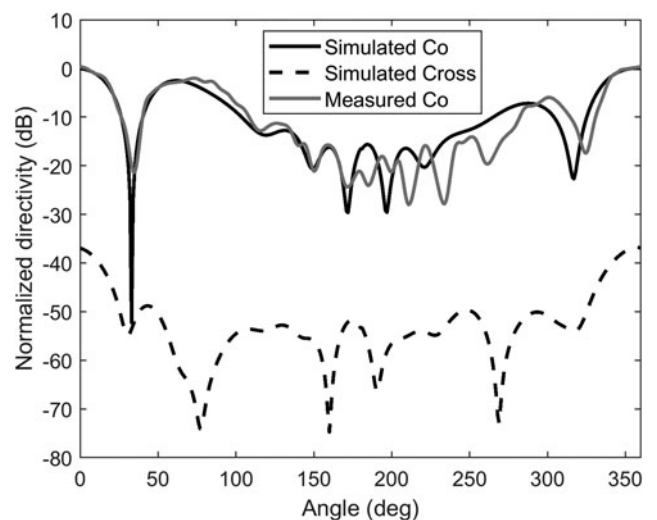
Fig. 22. Simulated and the measured radiation patterns of the implemented antenna in the E-plane.

radiation pattern fit the simulated radiation pattern well. The simulated cross-polarized radiation pattern of the designed antenna is also added to the figure which is approximately −40 dB below the co-polarization level at the main beam direction. The gain of the constructed antenna was measured, which was roughly equal to 13.5 dBi. The simulated gain of the antenna was equal to 14.1 dBi. The results and the performed discussion indicate that the proposed dumbbell-shaped slot antennas can be employed to design different types of slotted arrays. This enables a designer to design various types of arrays without
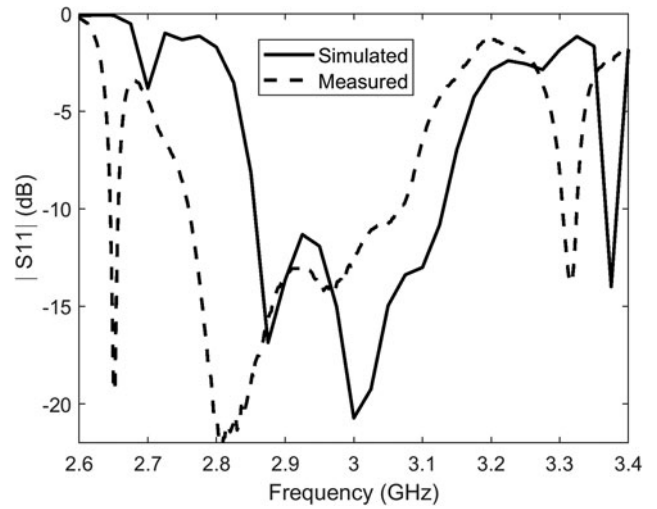
going through some tedious formulations or relying on trial-and-error procedure. The trial-and-error procedure usually requires the construction of several prototypes and near field measurements.

Conclusion

The dumbbell-shaped slot antennas were used as a replacement for round-ended longitudinal slot antennas. It was shown that by selecting an appropriate radius for the dumbbell ends, the resonant length is reduced dramatically. It has been observed that by employing such kind of slots in the planar arrays, the spacing between the edges of the nearest radiating slots to the junction and the edges of the coupling slots is increased. This increment forces the higher-order modes excited at the junctions to die out substantially before reaching the radiating slots. It was shown that employing the proposed dumbbell-shaped slot antennas enables one to neglect the effect of the higher-order mode in antenna designing equations, which saves time and manpower effort significantly.

References

1. **Elliott RS** (2003) *Antenna Theory and Design*, Revised Edn. Hoboken, NJ: John Wiley & Sons.
2. **Volakis J** (2007) *Antenna Engineering Handbook*, 4th Edn. New York: McGraw-Hill Education.
3. **Jasik H** (1961) *Antenna Engineering Handbook*. New York: McGraw-Hill.
4. **Lo YT and Lee SW** (1988) *Antenna Handbook: Theory, Applications, and Design*. New York: Van Nostrand Reinhold.
5. **Hirokawa J and Zhang M** (2014) Waveguide slot array antennas. In Chen ZN, (ed.), *Handbook of Antenna Technologies*. Singapore: Springer Singapore, pp. 1–21.
6. **Josefsson L and Rengarajan SR**. Slotted waveguide array antennas : theory, analysis and design. 2018.
7. **Sangster AJ** Compact slot array antennas for wireless communications. 2019.
8. **Silver S**, Engineers IoE. Microwave Antenna Theory and Design: P. Peregrinus; 1984.
9. **Kurtz L and Yee J** (1957) Second-order beams of two-dimensional slot arrays. *IRE Transactions on Antennas and Propagation* **5**, 356–362.
10. **McCormick G** (1958) The effect of the size of a two-dimensional array on the second-order beams. *IRE Transactions on Antennas and Propagation* **6**, 297–298.
11. **Gruenberg H** (1953) Second-order beams of slotted wave guide arrays. *Canadian Journal of Physics* **31**, 55–69.
12. **Derneryd A** Butterfly lobes in slotted waveguide antennas. 1987 Antennas and Propagation Society International Symposium: IEEE; 1987. pp. 360–363.
13. **Rengarajan SR and Steinbeck M** (1993) Longitudinal slots in dielectric-filled rectangular waveguides. *Microwave and Optical Technology Letters* **6**, 649–652.
14. **Casula GA, Mazzarella G and Montisci G** (2006) Design of slot arrays in waveguide partially filled with dielectric slab. *Electronics Letters* **42**, 730–731.
15. **Gatti RV, Sorrentino R and Dionigi M** Equivalent circuit of radiating longitudinal slots in dielectric filled rectangular waveguides obtained with FDTD method. 2002 IEEE MTT-S International Microwave Symposium Digest (Cat No 02CH37278): IEEE; 2002. pp. 871–874.
16. **Rengarajan S and Steinbeck M** Longitudinal slots in dielectric filled rectangular waveguides. Antennas and Propagation Society Symposium 1991 Digest: IEEE; 1991. pp. 1276–1279.
17. **Joubert J and McNamara D** (1991) Longitudinal slots in broad wall of rectangular waveguide inhomogeneously loaded with dielectric slab. *Electronics Letters* **27**, 1480–1482.
18. **Chatterjee S, Ghatak R and Poddar D** Analysis of asymmetric iris excited centered slot antenna on the broadwall of rectangular waveguide. ICIEE-2011. 2011.
19. **Park PK and Kim SH** Centered longitudinal shunt slot fed by a resonant offset ridge iris. Google Patents; 2001.
20. **Kim B-M, Hong J-P and Cho Y-K** (2016) Non-offset longitudinal shunt slot exited by an asymmetry compound iris. *The Journal of Korean Institute of Electromagnetic Engineering and Science* **27**, 684–692.
21. **Chatterjee S, Poddar DR and Majumder A** End fed iris excited centered slotted array antenna design with mutual coupling correction. 2013 International Conference on Microwave and Photonics (ICMAP): IEEE; 2013. pp. 1–5.
22. **Tang R** (1960) A slot with variable coupling and its application to a linear array. *IRE Transactions on Antennas and Propagation* **8**, 97–101.
23. **Chatterjee S, Poddar D and Ghatak R** Field Characterization of an iris excited 10 GHz slot radiator. TENCON 2011-2011 IEEE Region 10 Conference: IEEE; 2011. pp. 1127–1130.
24. **Goeffels F, Forman B and Nonnemaker C** (1968) Electronic scanning of linear slot arrays using diode irises. *IEEE Transactions on Antennas and Propagation* **16**, 380–381.
25. **Anand A and Das S** (2010) A novel virtually centered broad wall longitudinal slot for antenna application. *International Journal of RF and Microwave Computer-Aided Engineering: Co-sponsored by the Center for Advanced Manufacturing and Packaging of Microwave, Optical, and Digital Electronics (CAMPmode) at the University of Colorado at Boulder* **20**, 272–278.
26. **Chatterjee S, Poddar D and Ghatak R** Radiation characteristics of partial height curved iris excited centered slot X-band radiator. 2011 IEEE Applied Electromagnetics Conference (AEMC): IEEE; 2011. pp. 1–4.
27. **Mallahzadeh A and Mohammad-Ali-Nezhad S** (2015) A low cross-polarization slotted ridged SIW array antenna design with mutual coupling considerations. *IEEE Transactions on Antennas and Propagation* **63**, 4324–4333.
28. **Azar TJ**. Analysis of slotted-waveguide antenna array excited by tuning screws. PhDT. 1998:1775.
29. **Sing LK, Chet KV, Djuanda J and Sze LT** Analysis of slotted waveguide structure using MoM techniques. 4th National Conference of Telecommunication Technology, 2003 NCTT 2003 Proceedings: IEEE; 2003. pp. 40–44.
30. **Lim K-S, Koo V-C and Lim T-S** (2007) Design, simulation and measurement of a post slot waveguide antenna. *Journal of Electromagnetic Waves and Applications* **21**, 1589–1603.
31. **Green J, Shnitkin H and Bertalan PJ** (1990) Asymmetric ridge waveguide radiating element for a scanned planar array. *IEEE Transactions on Antennas and Propagation* **38**, 1161–1165.
32. **Moradian M, Khalaj-Amirhosseini M and Tayarani M** (2009) Application of wiggly ridge waveguide for design of linear array antennas of centered longitudinal shunt slot. *International Journal of RF and Microwave Computer-Aided Engineering: Co-sponsored by the Center for Advanced Manufacturing and Packaging of Microwave, Optical, and Digital Electronics (CAMPmode) at the University of Colorado at Boulder* **19**, 717–726.
33. **Moradian M, Tayarani M and Khalaj-Amirhosseini M** (2011) Planar slotted array antenna fed by single wiggly-ridge waveguide. *IEEE Antennas and Wireless Propagation Letters* **10**, 764–767.
34. **Moradian M** (2018) Planar slotted array antennas fed by reduced height wiggly ridge waveguides. *Journal of Electromagnetic Waves and Applications* **32**, 1232–1248.
35. **Moradian M and Hashemi S** (2018) Linear array of center line longitudinal slots excited by double ridge waveguides. *Radioengineering* **27**, 724–731.
36. **Khazai M and Khalaj-Amirhosseini M** (2016) To reduce side lobe level of slotted array antennas using nonuniform waveguides. *International Journal of RF and Microwave Computer-Aided Engineering* **26**, 42–46.
37. **Pesarakloo A, Sedighy SH and Hodjatkashani F** (2017) Sine-wall space-tapered linear slot array antenna with low sidelobe and second-order lobe levels. *IEEE Transactions on Antennas and Propagation* **66**, 1020–1024.

38. **Esmaeli S and Sedighy S** (2016) SLL Reduction of slot array antenna by artificial magnetic conductor side walls. *Electronics Letters* **52**, 1513–1514.

39. **Esmaeli S and Sedighy S** (2018) Application of artificial magnetic conductor metasurface for optimum design of slotted waveguide array antenna. *Applied Physics A* **124**, 136.

40. **Elliott R and O'Loughlin W** (1986) The design of slot arrays including internal mutual coupling. *IEEE Transactions on Antennas and Propagation* **34**, 1149–1154.

41. **Coetzee J and Joubert J** (1998) The effect of the inclusion of higher order internal coupling on waveguide slot array performance. *Microwave and Optical Technology Letters* **17**, 76–81.

42. **Shaw G, Rengarajan S and Elliott R** Analysis of mutual coupling in planar slot array antennas. IEEE Antennas and Propagation Society International Symposium 1992 Digest: IEEE; 1992. pp. 1480–1483.

43. **Rengarajan SR** (1991) Higher order mode coupling effects in the feeding waveguide of a planar slot array. *IEEE Transactions on Microwave Theory and Techniques* **39**, 1219–1223.

44. **Mazzarella G and Montisci G** (2011) Accurate modeling of coupling junctions in dielectric covered waveguide slot arrays. *Progress in Electromagnetics Research* **17**, 59–71.

45. **Rengarajan SR** (2012) Improved design procedure for slot array antennas using the method of moments analysis. *Electromagnetics* **32**, 221–232.

46. **Coetzee JC and Sheel S** (2018) Waveguide slot array design with compensation for higher order mode coupling between inclined coupling slots and neighboring radiating slots. *IEEE Transactions on Antennas and Propagation* **67**, 378–389.

47. **Kim B-M, Lee J-I and Cho Y-K** (2012) Ridge-loaded small round-ended slot for waveguide slot-array antenna. *The Journal of Korean Institute of Electromagnetic Engineering and Science* **23**, 950–957.

48. **Park P and Yu I** Characterization of Dumbbell Slots in Rectangular Waveguide by Method of Moments. 1985.

49. **Moradian M** (2019) Employing irises and septums to excite the centreline longitudinal slot antennas. *International Journal of RF and Microwave Computer-Aided Engineering* **29**, e21944.

50. **Stern G and Elliott R** (1985) Resonant length of longitudinal slots and validity of circuit representation: theory and experiment. *IEEE Transactions on Antennas and Propagation* **33**, 1264–1271.

51. **Moradian M** (2019) A computer-aided approach for designing dielectric-covered planar array antennas consisting of longitudinal slots. *International Journal of RF and Microwave Computer-Aided Engineering* **29**, e21615.

Mahdi Moradian obtained M.Sc. and Ph.D. both in electrical engineering from the Iran University of Science and Technology, Tehran, Iran, in 2004 and 2011, respectively. Since his graduation, he has worked in several institutes and universities as a lecturer and research engineer. He is interested in different areas of science and engineering, but currently, his main focus is on the slotted waveguide array antennas.